*Journal of Survey Statistics and Methodology (2023) **00**, 1–31*

POVERTY MAPPING UNDER AREA-LEVEL RANDOM REGRESSION COEFFICIENT POISSON MODELS

NAOMI DIZ-ROSALES
MARÍA JOSÉ LOMBARDÍA *
DOMINGO MORALES

Under an area-level random regression coefficient Poisson model, this article derives small area predictors of counts and proportions and introduces bootstrap estimators of the mean squared errors (MSEs). The maximum likelihood estimators of the model parameters and the mode predictors of the random effects are calculated by a Laplace approximation algorithm. Simulation experiments are implemented to investigate the behavior of the fitting algorithm, the predictors, and the MSE estimators with and without bias correction. The new statistical methodology is applied to data from the Spanish Living Conditions Survey. The target is to estimate the proportions of women and men under the poverty line by province.

KEY WORDS: Bootstrap; Poverty proportion; Random coefficient Poisson regression models; Small area estimation.

NAOMI DIZ-ROSALES is a Research Fellow and MARÍA JOSÉ LOMBARDÍA is Professor with the Universidade da Coruña, CITIC, A Coruña, Spain. DOMINGO MORALES is Professor with the Universidad Miguel Hernández de Elche, IUI-CIO, Elche, Spain.

This work was supported by the Ministry of Science and Innovation and the State Research Agency of the Spanish Government through the European Regional Development Fund (PID2022-136878NB-I00, PID2020-113578RB-I00 and PRE2021-100857 to Naomi Diz-Rosales funded by MCIN/AEI/10.13039/501100011033); by the Conselleria d'Innovació, Universitats, Ciéncia i Societat Digital of the Generalitat Valenciana (Prometeo/2021/063); by the Consellería de Cultura, Educación, Formación Profesional e Universidades of the Xunta de Galicia through the European Regional Development Fund (Competitive Reference Groups ED431C/2020/14, COV20/00604, and ED431G/2019/01); and by Centro de Investigación en Tecnologías de la Información y las Comunicaciones (CITIC) that is supported by Xunta de Galicia, collaboration agreement between the Consellería de Cultura, Educación, Formación Profesional e Universidades and the Galician universities for the reinforcement of the research centers of the Sistema Universitario de Galicia (CIGUS).

*Address correspondence to María José Lombardía, Universidade da Coruña, CITIC, Spain; E-mail: maria.jose.lombardia@udc.es.

https://doi.org/10.1093/jssam/smad036

Statement of significance

The main milestones achieved in this study are listed below:

- A Poisson area-level model with random regression coefficients is defined for the first time in small area estimation.
- The best predictors, their empirical versions, and their simplified versions, as well as the plug-in predictor for estimating poverty proportions are defined and evaluated under an area-level random regression coefficient Poisson model.
- The mean squared error of poverty proportion estimates is evaluated using parametric bootstrap estimators with and without bias correction.
- The developed methodology is applied to the study of poverty in Spain by province and sex, providing valuable poverty maps that demonstrate key socio-economic differences by geography.

1. INTRODUCTION

The United Nations (UN) has published that 10 percent of the world's population subsisted on less than $1.90 a day in 2015. Their projections for 2030 suggested that six percent of the population would continue to suffer extreme poverty. Since 2015, international policies have been guided by the 2030 Agenda and the 17 Sustainable Development Goals (SDGs). Within this common framework for action, the UN highlights the eradication of poverty as the first SDG. To achieve this goal, they point out the need to develop systems and strategies that ensure the social protection of citizens, with a focus on people who are below the poverty line and in a situation of particular vulnerability (United Nations 2022). However, the effectiveness of strategies is determined by an understanding of the structural socio-economic differences inherent in each country.

Poverty maps are established key tools in supporting policy decisions, as they facilitate analysis of the geographic distribution of poverty and the degree of inequality between the territories of a state. Consequently, policymakers require the estimation of these indicators at an increasingly lower level of aggregation, leading to potential degradation in precision and reliability. This deficiency can be addressed by small area estimation (SAE) methods that introduce model-based predictors for domains where the sample size is small and consequently direct estimators are imprecise. See Rao and Molina (2015) and Morales et al. (2021) for comprehensive introductions to SAE.

To estimate domain counts and proportions, SAE uses predictors based on area-level or unit-level linear mixed models (LMMs) and generalized linear mixed models (GLMMs). Area-level models are fitted to aggregated data that

may contain auxiliary variables from statistical sources other than the sample. Some examples of applications of area-level LMMs to poverty mapping are Esteban et al. (2012), Marhuenda et al. (2013, 2014), and Morales et al. (2015). Concerning GLMMs, binomial and multinomial mixed models for the estimation of proportions were applied by Molina et al. (2007), Ghosh et al. (2009), Chen and Lahiri (2012), Erciulescu and Fuller (2013), López-Vizcaíno et al. (2013, 2015), Berg and Fuller (2014), Militino et al. (2015), Chambers et al. (2016), Hobza and Morales (2016), Liu and Lahiri (2017), Hobza et al. (2018), as well as Franco and Bell (2022). The Poisson or Negative Binomial mixed models were employed to estimate counts or proportions by Tzavidis et al. (2015), Boubeta et al. (2016, 2017), Chandra et al. (2017, 2019), and Morales et al. (2022), among others. Zhang and Chambers (2004) proposed log-linear structural models for estimating cross-classified counts. Wang et al. (2018) and Esteban et al. (2020) proposed statistical models for compositional proportions.

All these above-cited papers assume that the slopes are fixed even though they may vary for certain groups of interest. In fact, Swamy (1970) and Demidenko (2013) noted that models with random regression coefficients are good research tools in the field of economics. Consequently, this article explores the use of area-level GLMMs with random coefficients in the SAE context.

Mixed models with random slopes were proposed by Dempster et al. (1981). Prasad and Rao (1990) gave empirical best linear unbiased predictors (EBLUPs) under a unit-level random regression coefficient LMM. They further derived second-order mean squared error (MSE) approximations and proposed analytical MSE estimators. Moura and Holt (1999) applied these models to household data from a county in Brazil to predict the Head of Household's income as a function of education level and number of rooms. Based on their simulation and implementation study results, they recommended allowing random slopes in the mixture models, noting that restricting random effects to intercepts does not capture variability as effectively. Hobza and Morales (2013) introduced unit-level LMMs with random coefficients to estimate average annual household income. Their simulation studies showed that incorporating random coefficients can improve the performance of EBLUPs. For longitudinal studies, chapter 13 of Morales et al. (2021) introduces LMMs with correlated random coefficients. In summary, there is substantive support in the statistical literature for including random regression coefficients in explanatory models when fitting models to "real" datasets. These same studies provide evidence against requiring fixed slopes in these same situations.

This article introduces a new statistical methodology for poverty mapping, illustrated by an application to data from the 2008 Spanish Living Condition Survey (SLCS). This survey is designed to obtain reliable direct estimators in NUTS 2-type regions (autonomous communities), but the sample sizes are quite small in NUTS 3-type territories (provinces), according to the current NUTS classification of EUROSTAT 2016. The target estimates are poverty proportions by sex in the Spanish provinces in 2008. Boubeta et al. (2017) addressed

this problem by modeling the counts of poor people as an area-level Poisson regression model with a random intercept. Building on this research, we propose a model with a random intercept and random slopes, specifically considering an area-level random regression coefficient Poisson model (ARRCP model). To assess this model, we develop a Laplace approximation algorithm to calculate the maximum likelihood (ML) estimators of the model parameters, derive model-based predictors of domain proportions, and present parametric bootstrap MSE estimators, each evaluated via extensive simulation studies.

The article is organized as follows. Section 2 describes the case study data and motivates the use of random slope models for better describing the target count variable. Section 3 introduces the area-level random regression coefficient Poisson model. Section 4 derives two predictors of domain proportions and counts: the empirical best predictor (EBP) and the plug-in predictor. Section 5 presents three simulation experiments patterned upon real data study case. The first simulation compares the statistical performance of the alternative predictors. The second simulation compares the statistical performance of the model with random slopes (and intercepts) against the model with only random intercepts (fixed slopes). The third simulation studies the behavior of the parametric bootstrap estimator of the MSE of the selected predictor with and without bias correction. Section 6 applies the new Poisson model to data from the 2008 SLCS. Section 7 gives some conclusions.

The article contains supplementary material. Appendix A in the supplementary data online describes the ML-Laplace fitting algorithm. Appendix B in the supplementary data online defines a simplified version of the EBP, the empirical simplified best predictor (BP). Appendix C in the supplementary data online develops three parametric bootstrap methods to estimate the MSE of predictors, two of them with bias correction. Appendix D in the supplementary data online presents four parametric bootstrap methods that can be used to calculate confidence intervals for model parameters. Appendix E in the supplementary data online carries out four additional simulation experiments that complement the results presented in section 5. Appendix F in the supplementary data online details the definition, characteristics, and selection of the ARRCP model in the application to real data.

2. DATA DESCRIPTION

The SLCS measures the incidence and composition of poverty by establishing a poverty risk threshold, providing information on the personal distribution of income based on net annual income, on household deprivation, and housing conditions and yields the harmonized indicator of risk of poverty or social exclusion. The SLCS is an annual statistic harmonized at the European level, carried out by the Spanish Statistical Office (INE—Instituto Nacional de Estadística). The data selected for this study correspond to the 2008 SLCS, with a sample size of

35,967. Although these data were collected 15 years ago, this data set is widely employed in the SAE literature of area-level models and is featured in the motivating research presented in Boubeta et al. (2017). Using the same dataset facilitates comparison between the different procedures without confounding and allows us to test model enhancements.

For the area-level models, we construct an aggregated data file with $D = 104$ domains defined by the crosses of the 52 Spanish provinces (including the cities of Ceuta and Melilla) and the two sexes. For each domain, the target variable of the Poisson model is the count of people with annual equivalized net incomes below a predetermined threshold established at 60 percent of the median income per consumption unit, indicated in euros (INE 2022). Auxiliary variables are taken from the 2008 Spanish Labour Force Survey (SLFS), whose covariates are related to the dependent variable (the number of poor people), a key requirement in SAE. The SLFS data on citizen participation in the labor is strongly associated with the characteristics of individual living conditions. Our auxiliary data choice is supported by the existing literature, with the numerous studies utilizing these auxiliary variables to estimate poverty indicators: see Molina and Rao (2010), Esteban et al. (2012), Molina et al. (2014), Morales et al. (2015), Benavent and Morales (2016, 2021), Boubeta et al. (2016), Marhuenda et al. (2017), or Boubeta et al. (2017), among others.

The SLFS is published quarterly by the INE. It has a much larger sample size than the SLCS, yielding reliable direct estimates in provinces. The auxiliary variables provided by the SLFS are the survey's direct estimates of the proportions of people in specific categories of unit-level factors. To increase the precision of the estimates, the four surveys of 2008 were combined. This avoids the problem of extending the area-level measurement error Poisson model of Morales et al. (2022) to the case of random regression coefficients.

Specifically, we consider the following unit-level categories:

Age (five categories):	$\leq$15 years old (age0)
	16–24 years old (age1)
	25–49 years old (age2)
	50–64 years old (age3)
	$\geq$65 years old (age4)

with age0 as the reference category.

Education (four categories):	$\leq$16 years old (edu0)
	Illiterate persons with incomplete or complete primary education and/or lower secondary education (edu1)

Persons with complete secondary education and/or postsecondary education such as baccalaureate or vocational training (edu2)

Persons with university studies (edu3)

with edu0 as the reference category.

Nationality (two categories): Spanish citizens including those with dual nationality (c)
Foreign citizenship (cit1)

with c as the reference category.

Labour status (four categories): ≤16 years (lab0)

Employed (lab1)

Unemployed (lab2)

Inactive (lab3)

with lab0 as the reference category.

Within each unit-level category, the sum of the proportions equals 1. To ensure unique parameters, we remove the selected reference category values from the data set.

To account for the divergence in the socio-economic structure of the Spanish provinces, we follow Tirado et al. (2016), introducing a variable that groups the provinces into clusters by their average income per household unit. The new variable, called *income group*, classifies the provinces into five clusters:

k=1 average household income of [20,484, 24,096) euros

k=2 average household income of [24,096, 26,206) euros

k=3 average household income of [26,206, 28,558) euro

k=4 average household income of [28,558, 31,364) euros

k=5 average household income of [31,364, 37,432) euros

That is, $k = 1$ includes the provinces with the lowest aggregated average incomes per household unit, whereas $k = 5$ includes those with the highest values. The definition of this variable, as well as a cluster sensitivity analysis, is extensively detailed in section F.1 in the supplementary data online.

Figure 1 examines the linear relationship between the logarithm of the sample poverty proportion and the auxiliary variables age3 (left) and lab2 (right) of the ARRCP model applied in section 6 (see table 4) for each of the five *income group* clusters. Note that (1) defines a logarithmic link, as natural for the Poisson distribution. Therefore, it makes sense to present the logarithm of the poverty proportion, as it is equivalent to the target natural parameter $\log p_{ij}$

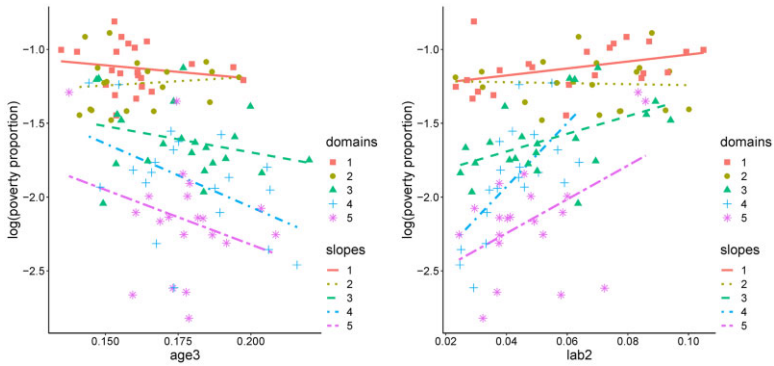

Figure 1. Log-Poverty-Proportion versus age3 and lab2 by Cluster $k, k=1, \cdots, 5$. The age3 variable represents the proportion of people who are 50–64 years old in the group income cluster k; the lab2 represents the proportion of unemployed persons in the group income cluster.

incorporated in that equation. Section F.1 in the supplementary data online presents similar figures for the remaining auxiliary variables. These figures show that slopes are not constant and vary by cluster k, $k = 1, \ldots, 5$.

The variable age3 represents the proportion of people aged 50–64. This stage is characterized by professional stability, with privileges achieved after a long career in the labor market. We therefore expect to observe a decreasing slope for each income group (cluster), logically reasoning that provinces with higher proportions of people in this age range should exhibit lower proportions of poverty. Indeed, this is the case for all groups, with the exception of $k = 2$, which has a notably less steep slope than the other income groups and exhibits a slightly positive trend visually. This cluster comprises a variety of provinces. On the one hand, it includes "Empty Spain" territories such as Lugo, where the population is markedly aged. In such populations, job offers tend to be associated with optimal conditions, regardless of age group. This group also includes the autonomous city of Ceuta, whose combined estimates with Melilla have a significantly greater sampling error than the rest of Spain according to the INE.

The variable lab2 represents the proportion of unemployed people. We expect positive slopes in each income group cluster, since provinces with a greater proportion of unemployed population will tend to have greater proportions of poverty. This is confirmed in all clusters, with particularly steep slopes in the greater income groups of provinces ($k = 4$ and $k = 5$), except in the cluster $k = 2$, which exhibits a nearly virtually constant slope. Figure 1 shows clear differences in slopes by income group cluster for the age3 and lab2 variables, with especially pronounced differences with the lab2 variable, which has crossed slopes in clusters k=4 and k=5. The age3 variable likewise shows differences in slope by income group cluster, albeit to a lesser extent. Consequently, we

posited that the random coefficient associated with the unemployment indicator variable should explain a large component of the variance of the Poisson model.

Figure 1 and appendix F.1.3 in the supplementary data online demonstrate deficiencies in area-level Poisson mixed model whose only random effect is the intercept. This model does not capture all the variability of the current aggregated poverty data, providing visual evidence for incorporating a random slope coefficient by income groups. Consequently, the following section defines the empirical new Poisson model that will be used in the application presented in Section 6.

3. THE ARRCP MODEL

This section introduces the new ARRCP model, along with all necessary notation. Let y_{ij} be a count variable taking values on $\mathbb{N} \cup \{0\}$, where $i \in \mathbb{I} = \{1, \ldots, I\}$ and $j \in \mathbb{J} = \{1, \ldots, J\}$. Let $D = IJ$ be the total number of y values. In our application, y_{ij} is the number of people below the poverty threshold in a survey sample, the indexes i and j represent province and sex, and D is the total number of domains defined by crossing of the variables province and sex. We classify each provide into one of K income group clusters, $\mathbb{I}_1, \ldots, \mathbb{I}_K$ with $k(i)$ designating the specific cluster assignment for province i, $k(i) \in \mathbb{K} = \{1, \ldots, K\}$. The number of provinces in the cluster $\mathbb{I}_k$ is $m_k = \#(\mathbb{I}_k)$, so that $D = J \sum_{k=1}^{K} m_k$. As a particular case, we could consider no clustering, with $m_k = 1$ for $k(i) \in \mathbb{K} = \{1, \ldots, K\}$, where $K = I$.

We use this area-level data to model and predict the target variable y_{ij}. Assume that there are p explanatory variables with values $x_{\ell,ij}$, $\ell \in \mathbb{P} = \{1, \ldots, p\}$, $i \in \mathbb{I}$, $j \in \mathbb{J}$. For models that include an intercept, we take $x_{1,ij} = 1$ for all i and j. Hereafter, we present the area-level random regression coefficient Poisson model that is ultimately applied to empirical poverty data in section 6.

Let u_{ij}, $i \in \mathbb{I}$, $j \in \mathbb{J}$ be i.i.d. $N(0, 1)$ random variables. Let $\phi_\ell > 0$ $(\ell \in \mathbb{P})$ be unknown standard deviation parameters. Let $\rho_{rs} \in (-1, 1)$ $(r < s,\ r, s \in \mathbb{P})$ be unknown correlation parameters. Let $\boldsymbol{v}_k = \left(v_{1,k}, \ldots, v_{p,k}\right)'(k \in \mathbb{K})$ be i.i.d. random vectors such that

$$\underset{1 \le \ell \le p}{\text{diag}}\ (\phi_\ell)\boldsymbol{v}_k \sim N_p\left(0, \boldsymbol{V}_{vk}^{\phi}\right),$$

$$\boldsymbol{V}_{vk}^{\phi} = \begin{pmatrix} \phi_1^2 & \phi_1\phi_2\rho_{12} & \cdots & \phi_1\phi_p\rho_{1p} \\ \phi_2\phi_1\rho_{12} & \phi_2^2 & \cdots & \phi_2\phi_p\rho_{2p} \\ \vdots & \vdots & \ddots & \vdots \\ \phi_p\phi_1\rho_{1p} & \phi_p\phi_2\rho_{2p} & \cdots & \phi_p^2 \end{pmatrix}.$$

Therefore, the variance matrix of $\boldsymbol{v}_k$ is

$$\boldsymbol{V}_{vk} = \mathrm{var}(\boldsymbol{v}_k) = \underset{1 \le \ell \le p}{\mathrm{diag}} \left(\phi_\ell^{-1}\right) \boldsymbol{V}_{vk}^{\phi} \underset{1 \le \ell \le p}{\mathrm{diag}} \left(\phi_\ell^{-1}\right) = \begin{pmatrix} 1 & \rho_{12} & \dots & \rho_{1p} \\ \rho_{12} & 1 & \dots & \rho_{2p} \\ \vdots & \vdots & \ddots & \vdots \\ \rho_{1p} & \rho_{2p} & \dots & 1 \end{pmatrix}.$$

Define the matrix $\boldsymbol{V}_v = \mathrm{diag}_{1 \le k \le K} (\boldsymbol{V}_{vk})$ and the vectors

$$\boldsymbol{u} = \underset{1 \le i \le I}{\mathrm{col}} \left(\underset{1 \le j \le J}{\mathrm{col}} \left(u_{ij}\right) \right) \sim N_D(\boldsymbol{0}, \boldsymbol{I}_D), \quad \boldsymbol{v} = \underset{1 \le k \le K}{\mathrm{col}} (\boldsymbol{v}_k) \sim N_{pK}(\boldsymbol{0}, \boldsymbol{V}_v),$$

where diag and col are the diagonal and the column operator, respectively. We assume that $\boldsymbol{u}$ and $\boldsymbol{v}$ are independent. The distribution of the target variable y_{ij}, conditioned to the random effects u_{ij}, $v_{\ell,k(i)}$ $\left(\ell \in \mathbb{P}\right)$ is

$$y_{ij} | u_{ij}, v_{1,k(i)}, \dots, v_{p,k(i)} \sim \mathrm{Poisson}\left(\nu_{ij} p_{ij}\right), \quad i \in \mathbb{I}, j \in \mathbb{J},$$

where the offset parameters $\nu_{ij} > 0$ are known and correspond to the sample size when the model is applied to real data, and the binomial probability p_{ij} is the target parameter with range (0,1).

For the natural parameters, we assume

$$\begin{aligned} \eta_{ij} &= \log \mu_{ij} = \log \nu_{ij} + \log p_{ij} \\ &= \log \nu_{ij} + \sum_{\ell=1}^{p} \beta_\ell x_{\ell,ij} + \sigma u_{ij} + \sum_{\ell=1}^{p} \phi_\ell v_{\ell,k(i)} x_{\ell,ij}, i \in \mathbb{I}, j \in \mathbb{J}, \end{aligned} \tag{1}$$

where $\mu_{ij} = E\left[y_{ij} | u_{ij}, v_{1,k(i)}, \dots, v_{p,k(i)}\right]$. We may write $\boldsymbol{x}_{ij}\boldsymbol{\beta} = \sum_{\ell=1}^{p} \beta_\ell x_{\ell,ij}$, where $\boldsymbol{\beta} = \mathrm{col}_{1 \le \ell \le p} (\beta_\ell)$ is the column vector of regression parameters and $\boldsymbol{x}_{ij} = \mathrm{col}'_{1 \le \ell \le p} \left(x_{\ell,ij}\right)$ is the row vector of known auxiliary variables. To finish the definition of the ARRCP model, we assume that the y_{ij}s are independent conditioned on $\boldsymbol{u}$ and $\boldsymbol{v}$. The variance component parameters are $\sigma > 0$, $\boldsymbol{\phi} = \left(\phi_1, \dots, \phi_p\right)' \in \mathbb{R}_+^p$, and $\boldsymbol{\rho} = \left(\rho_{12}, \dots, \rho_{1p}, \dots, \rho_{p-1p}\right)' \in (-1,1)^{p(p-1)/2}$, where $\mathbb{R}_+ = (0, \infty)$. The vector of model parameters is $\boldsymbol{\theta} = (\boldsymbol{\beta}', \sigma, \boldsymbol{\phi}', \boldsymbol{\rho}')'$. The total number of random effects is $H = D + pK$. Define

$$\boldsymbol{y}_i = \underset{1 \le j \le J}{\mathrm{col}} \left(y_{ij}\right), i \in \mathbb{I}, \quad \boldsymbol{y} = \underset{1 \le i \le I}{\mathrm{col}} (\boldsymbol{y}_i), \quad c(\boldsymbol{y}) = (2\pi)^{-\frac{H}{2}} \prod_{i=1}^{I} \prod_{j=1}^{J} \left(\nu_{ij}^{y_{ij}} / y_{ij}!\right).$$

It holds that

$$P\left(y_{ij}|\boldsymbol{u},\boldsymbol{v};\boldsymbol{\theta}\right) = P\left(y_{ij}|u_{ij},v_{\ell,k(i)}\right) = \frac{1}{y_{ij}!}\exp\left\{-\nu_{ij}p_{ij}\right\}\nu_{ij}^{y_{ij}}p_{ij}^{y_{ij}},$$

$$p_{ij} = \exp\left\{\boldsymbol{x}_{ij}\boldsymbol{\beta} + \sigma u_{ij} + \sum_{\ell=1}^{p}\phi_\ell v_{\ell,k(i)}x_{\ell,ij}\right\},$$

$$P(\boldsymbol{y}|\boldsymbol{u},\boldsymbol{v};\boldsymbol{\theta}) = \prod_{i=1}^{I}\prod_{j=1}^{J}P\left(y_{ij}|\boldsymbol{u},\boldsymbol{v};\boldsymbol{\theta}\right),$$

$$P(\boldsymbol{y};\boldsymbol{\theta}) = \int_{\mathbb{R}^H}P(\boldsymbol{y}|\boldsymbol{u},\boldsymbol{v};\boldsymbol{\theta})f_u(\boldsymbol{u})f_v(\boldsymbol{v})d\boldsymbol{u}d\boldsymbol{v} = \int_{\mathbb{R}^H}\psi(\boldsymbol{y},\boldsymbol{u},\boldsymbol{v};\boldsymbol{\theta})d\boldsymbol{u}d\boldsymbol{v},$$

where

$$\psi(\boldsymbol{y},\boldsymbol{u},\boldsymbol{v};\boldsymbol{\theta}) = (2\pi)^{-\frac{H}{2}}\exp\left\{-\frac{1}{2}\boldsymbol{u}'\boldsymbol{u}\right\}|\boldsymbol{V}_v|^{-1/2}\exp\left\{-\frac{1}{2}\boldsymbol{v}'\boldsymbol{V}_v^{-1}\boldsymbol{v}\right\}\prod_{i=1}^{I}\prod_{j=1}^{J}\frac{\exp\left\{-\nu_{ij}p_{ij}\right\}\nu_{ij}^{y_{ij}}p_{ij}^{y_{ij}}}{y_{ij}!}$$

$$= c(\boldsymbol{y})\exp\left\{-\frac{1}{2}\boldsymbol{u}'\boldsymbol{u}\right\}|\boldsymbol{V}_v|^{-1/2}\exp\left\{-\frac{1}{2}\boldsymbol{v}'\boldsymbol{V}_v^{-1}\boldsymbol{v}\right\}$$

$$\cdot\exp\left\{-\sum_{i=1}^{I}\sum_{j=1}^{J}\nu_{ij}\exp\left\{\boldsymbol{x}_{ij}\boldsymbol{\beta}+\sigma u_{ij}+\sum_{\ell=1}^{p}\phi_\ell v_{\ell,k(i)}x_{\ell,ij}\right\}\right\}$$

$$\cdot\exp\left\{\sum_{\ell=1}^{p}\left(\sum_{i=1}^{I}\sum_{j=1}^{J}y_{ij}x_{\ell,ij}\right)\beta_\ell+\sum_{i=1}^{I}\sum_{j=1}^{J}\left\{\sigma u_{ij}+\sum_{\ell=1}^{p}\phi_\ell v_{\ell,k(i)}x_{\ell,ij}\right\}y_{ij}\right\}.$$

Given $\boldsymbol{y}$, the ML estimator of $\boldsymbol{\theta}$ is

$$\hat{\boldsymbol{\theta}} = \text{argmax}_{\theta\in\Theta}P(\boldsymbol{y};\boldsymbol{\theta}), \quad \Theta = \mathbb{R}^p\times\mathbb{R}_+^{p+1}\times(-1,1)^{p(p-1)/2}.$$

To carry out the maximization, we iteratively apply an R function to approximate the integral in $\mathbb{R}^H$ and an R function for optimization. Alternatively, one could use the Laplace approximation algorithm derived in appendix A discussed in the supplementary data online. Similarly, one could use the accompanying asymptotic confidence intervals and p-values for to evaluate the model parameters or use the bootstrap confidence intervals described in appendix D of the supplementary data online.

4. PREDICTORS

This section derives predictors of p_{ij} and μ_{ij} under the ARRCP model. Definte

$$\boldsymbol{y}_{jk} = \underset{i\in\mathbb{I}_k}{\text{col}}\left(y_{ij}\right), \quad \boldsymbol{u}_{jk} = \underset{i\in\mathbb{I}_k}{\text{col}}\left(u_{ij}\right).$$

The conditional distribution of $\boldsymbol{y}$, given $\boldsymbol{u}$ and $\boldsymbol{v}$, is

$$P(\boldsymbol{y}|\boldsymbol{u},\boldsymbol{v}) = \prod_{j=1}^{J}\prod_{k=1}^{K} P\left(\boldsymbol{y}_{jk}|\boldsymbol{u},\boldsymbol{v}\right) = \prod_{j=1}^{J}\prod_{k=1}^{K} P\left(\boldsymbol{y}_{jk}|\boldsymbol{u}_{jk},\boldsymbol{v}_k\right),$$

$$P\left(\boldsymbol{y}_{jk}|\boldsymbol{u}_{jk},\boldsymbol{v}_k\right) = \prod_{i\in\mathbb{I}_k} P\left(y_{ij}|\boldsymbol{u}_{jk},\boldsymbol{v}_k\right) = \prod_{i\in\mathbb{I}_k} P\left(y_{ij}|u_{ij},\boldsymbol{v}_k\right),$$

where

$$\begin{aligned} P\left(y_{ij}|u_{ij},\boldsymbol{v}_{k(i)}\right) &= \frac{1}{y_{ij}!}\exp\left\{-\nu_{ij}p_{ij}\right\}\nu_{ij}^{y_{ij}}p_{ij}^{y_{ij}} \\ &= c_{ij}\exp\left\{y_{ij}\quad \boldsymbol{x}_{ij}\boldsymbol{\beta} + \sigma u_{ij} + \sum_{\ell=1}^{p}\phi_\ell v_{\ell,k(i)}x_{\ell,ij}\right) \\ &\quad -\nu_{ij}\exp\left\{\boldsymbol{x}_{ij}\boldsymbol{\beta} + \sigma u_{ij} + \sum_{\ell=1}^{p}\phi_\ell v_{\ell,k(i)}x_{\ell,ij}\right\}\right\} \end{aligned}$$

and $c_{ij} = 1/\left(y_{ij}!\right)\nu_{ij}^{y_{ij}}$. The p.d.f. of $\boldsymbol{u}_{jk}$ and $\boldsymbol{v}_k$ are

$$f_v(\boldsymbol{v}_k) = (2\pi)^{-\frac{p}{2}}|\boldsymbol{V}_{vk}|^{-1/2}\exp\left\{-\frac{1}{2}\boldsymbol{v}_k'\boldsymbol{V}_{vk}^{-1/2}\boldsymbol{v}_k\right\} \sim N_p(\boldsymbol{0},\boldsymbol{V}_{vk}),$$

$$f_u\left(\boldsymbol{u}_{jk}\right) = (2\pi)^{-\frac{m_k}{2}}\exp\left\{-\frac{1}{2}\boldsymbol{u}_{jk}'\boldsymbol{u}_{jk}\right\} \sim N_{m_k}(\boldsymbol{0},\boldsymbol{I}_{m_k}).$$

Recall that p_{ij} only depends on u_{ij} and $\boldsymbol{v}_{k(i)}$, and that the random effects u_{ij} and $\boldsymbol{v}_k$, $i\in\mathbb{I}$, $j\in\mathbb{J}$, $k\in\mathbb{K}$ are independent. Therefore, the components of $\boldsymbol{y}$ that are not in $\boldsymbol{y}_{jk(i)}$ are independent of p_{ij}. However, p_{ij} is not independent of $\boldsymbol{y}_{jk(i)}$.

The BP of p_{ij} is

$$\hat{p}_{ij}^{\text{bp}} = \hat{p}_{ij}^{\text{bp}}(\boldsymbol{\theta}) = E_\theta\big[p_{ij}|\boldsymbol{y}\big] = E_\theta\Big[p_{ij}|\boldsymbol{y}_{jk(i)}\Big] = \frac{A_{ij}}{B_{k(i)}},$$

$$A_{ij} = \int_{R^{p+m_k}} \exp\left\{\boldsymbol{x}_{ij}\boldsymbol{\beta} + \sigma u_{ij} + \sum_{\ell=1}^{p}\phi_\ell v_{\ell,k(i)}x_{\ell,ij}\right\}.$$

$$P\Big(\boldsymbol{y}_{jk(i)}|\boldsymbol{u}_{jk(i)}, \boldsymbol{v}_{k(i)}\Big)f_u\big(\boldsymbol{u}_{jk(i)}\big)f_v\big(\boldsymbol{v}_{k(i)}\big)d\boldsymbol{u}_{jk(i)}d\boldsymbol{v}_{k(i)},$$

$$B_{k(i)} = \int_{R^{p+m_k}} P\Big(\boldsymbol{y}_{jk(i)}|\boldsymbol{u}_{jk(i)}, \boldsymbol{v}_{k(i)}\Big)f_u\big(\boldsymbol{u}_{jk(i)}\big)f_v\big(\boldsymbol{v}_{k(i)}\big)d\boldsymbol{u}_{jk(i)}d\boldsymbol{v}_{k(i)}.$$

The EBP of p_{ij} is $\hat{p}_{ij}^{\text{ebp}} = \hat{p}_{ij}^{\text{bp}}\left(\hat{\boldsymbol{\theta}}\right)$ and the EBP of $\mu_{ij} = v_{ij}p_{ij}$ is $\hat{\mu}_{ij}^{\text{ebp}} = v_{ij}\hat{p}_{ij}^{\text{ebp}}$. The EBP $\hat{p}_{ij}^{\text{ebp}}$ can be approximated by the following Monte Carlo method:

(1) Estimate $\hat{\boldsymbol{\theta}} = \left(\hat{\boldsymbol{\beta}}', \hat{\sigma}, \hat{\boldsymbol{\phi}}', \hat{\boldsymbol{\rho}}'\right)'$. Set $k = k(i)$.
(2) For $s_1 = 1, \ldots, S_1$, $s_2 = 1, \ldots, S_2$, generate $\boldsymbol{u}_{jk}^{(s_1)} \sim N_{m_k}(0, \boldsymbol{I}_{m_k})$, $\boldsymbol{v}_k^{(s_2)} \sim N_p\big(0, \hat{\boldsymbol{V}}_{vk}\big)$ and $\boldsymbol{u}_{jk}^{(S_1+s_1)} = -\boldsymbol{u}_{jk}^{(s_1)}$, $\boldsymbol{v}_k^{(S_2+s_2)} = -\boldsymbol{v}_k^{(s_2)}$, where $\hat{\boldsymbol{V}}_{vk} = \boldsymbol{V}_{vk}(\hat{\boldsymbol{\rho}})$.
(3) Calculate $\hat{p}_{ij}^{\text{ebp}} = \hat{A}_{ij}/\hat{B}_{k(i)}$, where

$$\hat{A}_{ij} = \sum_{s_1=1}^{2S_1}\sum_{s_2=1}^{2S_2}\exp\left\{\sum_{r\in\mathbb{I}_k}\left\{\big(y_{rj} + \delta_{ri}\big)\ \boldsymbol{x}_{rj}\hat{\boldsymbol{\beta}} + \hat{\sigma}u_{rj}^{(s_1)} + \sum_{\ell=1}^{p}\hat{\phi}_\ell v_{\ell,k}^{(s_2)}x_{\ell,rj}\right)\right.$$
$$\left.-v_{rj}\exp\left\{\boldsymbol{x}_{rj}\hat{\boldsymbol{\beta}} + \hat{\sigma}u_{rj}^{(s_1)} + \sum_{\ell=1}^{p}\hat{\phi}_\ell v_{\ell,k}^{(s_2)}x_{\ell,rj}\right\}\right\}\right\},$$

$$\hat{B}_{k(i)} = \sum_{s_1=1}^{2S_1}\sum_{s_2=1}^{2S_2}\exp\left\{\sum_{r\in\mathbb{I}_k}\left\{y_{rj}\ \ \boldsymbol{x}_{rj}\hat{\boldsymbol{\beta}} + \hat{\sigma}u_{rj}^{(s_1)} + \sum_{\ell=1}^{p}\hat{\phi}_\ell v_{\ell,k}^{(s_2)}x_{\ell,rj}\right)\right.$$
$$\left.-v_{rj}\exp\left\{\boldsymbol{x}_{rj}\hat{\boldsymbol{\beta}} + \hat{\sigma}u_{rj}^{(s_1)} + \sum_{\ell=1}^{p}\hat{\phi}_\ell v_{\ell,k}^{(s_2)}x_{\ell,rj}\right\}\right\}\right\},$$

and δ_{ri} is the delta of Kronecker, that is, $\delta_{ri} = 1$ if $r = i$ and $\delta_{ri} = 0$ if $r \neq i$.

The EBPs are usually computationally demanding and are not necessarily unbiased. Another option is to consider the computationally simpler plug-in predictor of p_{ij}, which has the form

$$\hat{p}_{ij}^{\text{in}} = \exp\left\{\boldsymbol{x}_{ij}\hat{\boldsymbol{\beta}} + \hat{\sigma}\hat{u}_{ij} + \sum_{\ell=1}^{p}\hat{\phi}_\ell\hat{v}_{\ell,k(i)}x_{\ell,ij}\right\}, \tag{2}$$

where $\hat{u}_{ij}$ and $\hat{v}_{\ell,k(i)}$, $\ell = 1, \ldots, p$, are the mode predictors taken from the output of the ML-Laplace algorithm. The plug-in predictor of $\mu_{ij} = v_{ij}p_{ij}$ is $\hat{\mu}_{ij}^{\text{in}} = v_{ij}\hat{p}_{ij}^{\text{in}}$.

5. SIMULATIONS

This section presents three simulation experiments, applying the AARCP model defined in section 3 to simulated data modeled after the empirical data used in section 6. Simulation 1 compares the performance of the predictors introduced in section 4. Simulation 2 compares the behavior of plug-in predictors obtained with the ARRCP model (model 1) to that obtained using a model whose random effects are restricted to intercepts (model 0), with the target data are generated from either model (0 or 1). Simulation 3 evaluates the behavior of the parametric bootstrap estimators of the MSEs of the plug-in predictors; see appendix C in the supplementary data online.

Using the aggregated data file described in section 2 as predictors, we simulated the dependent variable y_{ij} for each province i and sex j, using the regression and variance parameters obtained from the empirical application of the ARRCP presented in section 6.

The domain target parameter p_{ij} corresponds to the domain proportion of people below the poverty threshold. The model contains $p = 5$ auxiliary variables: $x_1 =$ intercept, $x_2 =$ age3, $x_3 =$ edu1, $x_4 =$ cit1, and $x_5 =$ lab2, with regression parameters $\beta_1 = -1.3806$, $\beta_2 = -4.2120$, $\beta_3 = 1.0048$, $\beta_4 = -1.3491$, and $\beta_5 = 6.9135$. The standard deviation parameters are $\sigma = 0.1414$, $\phi_1 = 0$, $\phi_2 = 2.0617$, $\phi_3 = 0$, $\phi_4 = 0$, and $\phi_5 = 2.5985$. The correlation parameters are $\rho_{25} = -0.9432$ and $\rho_{ab} = 0$ for any other $a < b$ belonging to the set $\mathbb{K} = \{1, 2, 3, 4, 5\}$. The natural parameter of the selected ARRCP model is

$$\begin{aligned}\log \mu_{ij} &= \log \nu_{ij} + \log p_{ij} \\ &= \log \nu_{ij} + \sum_{\ell=1}^{5} \beta_\ell x_{\ell,ij} + \sigma u_{ij} + \phi_2 v_{2,k(i)} x_{2,ij} + \phi_5 v_{5,k(i)} x_{5,ij},\end{aligned}$$

where $\nu_{ij} = n_{ij}$ is the sample size in province i and sex j, $u_{ij} \sim N(0,1)$, $(v_{2,k}, v_{5,k})' \sim N_2(\mathbf{0}, \boldsymbol{V}_{25})$, $\mathbf{0} = (0,0)'$ and $\boldsymbol{V}_{25}(\rho_{25}) = \begin{pmatrix} 1 & \rho_{25} \\ \rho_{25} & 1 \end{pmatrix}$. [Note that model 0 is a particular case of the ARRCP model, where $\phi_2 = \phi_5 = \rho_{25} = 0$.] To approximate the BP and the EBP, we take $S_1 = S_2 = 2,500$ in the Monte Carlo algorithm given in section 4.

Appendix E in the supplementary data online outlines four additional complementary simulation experiments.

5.1 Simulation 1

Simulation 1 evaluates the respective performance of the BP, EBP, and plug-in predictors over repeated samples. To perform the simulation, we:

(1) Repeat the following steps $R = 1{,}000$ times ($r = 1, \ldots, R$):

1.1 Generate $u_{ij}^{(r)}$ i.i.d. $N(0, 1)$ and $\boldsymbol{v}_k^{(r)}$ i.i.d. $N_p(\mathbf{0}, \boldsymbol{V}_{25}(\rho_{25}))$, $i \in \mathbb{I}, j \in \mathbb{J}$, $k \in \mathbb{K}$.

1.2 Calculate $p_{ij}^{(r)} = \exp\{\boldsymbol{x}_{ij}\boldsymbol{\beta} + \sigma u_{ij}^{(r)} + \phi_2 v_{2,k(i)}^{(r)} x_{2,ij} + \phi_5 v_{5,k(i)}^{(r)} x_{5,ij}\}$, $i \in \mathbb{I}, j \in \mathbb{J}$.

1.3 Generate $y_{ij}^{(r)} = \text{Poisson}(v_{ij} p_{ij}^{(r)})$, $i \in \mathbb{I}, j \in \mathbb{J}$.

1.4 Calculate $\hat{\tau}^{(r)} \in \{\beta_1, \ldots, \beta_5, \sigma, \phi_2, \phi_5, \rho_{25}\}$ and $\hat{p}_{ij}^{m(r)}$ for all $j \in \mathbb{J}$ where $m =$ BP, EPB, and IN (the plug-in estimator).

(2) For each prediction method m, calculate

Bias (within): $BIAS_{ij}^m = \frac{1}{R}\sum_{r=1}^{R}\left(\hat{p}_{ij}^{m(r)} - p_{ij}^{(r)}\right)$

Absolute Bias: $ABIAS^m = \frac{1}{IJ}\sum_{i=1}^{I}\sum_{j=1}^{J}\left|BIAS_{ij}^m\right|$

Root-MSE (within): $RMSE_{ij}^m = \left[\frac{1}{R}\sum_{r=1}^{R}\left(\hat{p}_{ij}^{m(r)} - p_{ij}^{(r)}\right)^2\right]^{1/2}$

Root-MSE: $RMSE^m = \frac{1}{IJ}\sum_{i=1}^{I}\sum_{j=1}^{J} RMSE_{ij}^m$

(3) Calculate the corresponding relative performance measures (in percent):

Relative Bias (within): $RBIAS_{ij}^m = 100 \times \left(\frac{BIAS_{ij}^m}{\bar{p}_{ij}}\right)$

Relative RMSE (within): $RRMSE_{ij}^m = 100 \times \left(\frac{RMSE_{ij}^m}{\bar{p}_{ij}}\right)$

Absolute Relative Bias: $ARBIAS^m = \frac{1}{IJ}\sum_{i=1}^{I}\sum_{j=1}^{J}\left|RBIAS_{ij}^m\right|$

Relative Root-MSE: $RRMSE^m = \frac{1}{IJ}\sum_{i=1}^{I}\sum_{j=1}^{J} RRMSE_{ij}^m$

where $\bar{p}_{ij} = \frac{1}{R}\sum_{r=1}^{R} p_{ij}^{(r)}$

Table 1 shows the absolute and relative performance measures in percent for the BP, the EBP, and for the plug-in (IN). Also, for a more in-depth analysis, figure 2 illustrates the performance of the EBP and plug-in predictions in terms of BIAS_{ij} (left) and RMSE_{ij} (right) for each domain, plotted in ascending order of sample size.

Considering these results collectively, we note the following. First, the BP consistently outperforms the EBP in terms of bias and precision. However, the relative performances of these two approaches are not markedly different, despite the parameter estimation effects with the EPB. Second, the EBP predictions should (in theory) have similar properties to those of the BP, as the EBP is unbiased predictor that minimizes the MSE. This is not borne out by the

Table 1. Performance Measures for Predictors

	BP	EBP	IN
10^3 ABIAS	0.6119	0.7042	0.6119
10^3 RMSE	25.5329	26.1465	23.1661
ARBIAS	0.2850	0.3339	0.2851
RRMSE	11.5156	11.7813	10.4189

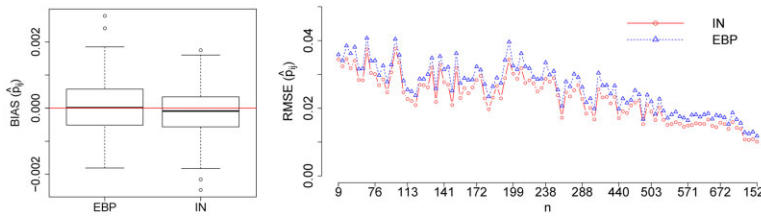

Figure 2. BIAS (Left) and RMSE (Right) of $\hat{p}_{ij}$ Ordered by Sample Size.

results. In fact, the biases of corresponding BP and plug-in estimates have similar magnitude, whereas the EPB biases are larger. In addition, the plug-in predictor has lower RMSE compared to the other predictors. As expected, the EPB is unbiased, whereas the plug-in estimator is slightly negatively biased; see the boxplot on the left. On the other hand, the plug-in predictor is considerably less variable, with the EPB variability increasing as the sample size decreases.

Recall that we generated $S_1 = S_2 = 2,500$ random variables to approximate the BP of p_{ij}. This predictor requires approximating a multiple integral of dimension $p + m_k$, where p is the number of parameters, and m_k the number of domains in each cluster k (between 20 and 22 domains per cluster). The BP incorporates the Monte Carlo variance, which is high, and has a starting variance underlying the integral estimation; an optimal approximation would require at least 10,000 iterations. Thus, not only is this problem mathematically complex, it is computationally very expensive. This simulation required about nine days of computation time to obtain the BP and EBP estimates.

The plug-in predictor is by definition biased, since its unbiasedness properties are related to linear functions, and the objective is exponential. However, the bias is not markedly different from that with the EBP, as shown in figure 2. Figure 3 plots the plug-in model predictions obtained with (2) against the simulated values. Notice that the deviation from linearity is not strong in this specific data set. Consequently, although the tendency of all the considered predictors decrease the RMSE_{ij} as the sample sizes increase, we use the plug-in predictor for our real data application, as it best balances performance and computational efficiency.

5.2 Simulation 2

Simulation 2 compares the behavior of the plug-in predictors of p_{ij} based on model 0 (random intercepts) and on model 1 (random intercepts and slopes), denoted by $\hat{p}_{ij}^{\text{in0}}$ (IN0) and $\hat{p}_{ij}^{\text{in1}}$ (IN1) respectively. We follow the steps outlined in simulation 1, but generate two sets of data (one under model 1, one under model 0), calculating both predictors IN0 and IN1 in each data set. If either model fails to converge, the iteration is discarded and and replaced by a new one as advised by Matuschek et al. (2017).

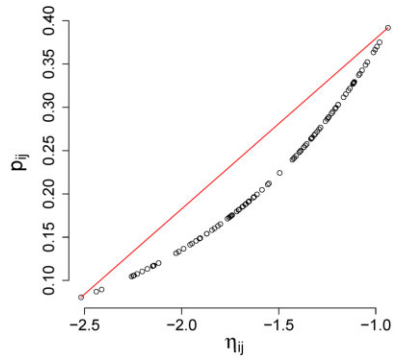

Figure 3. Linear Predictor η_{ij} versus p_{ij}.

If model 1 is the true generating model, then the best performance (i.e., lowest bias and root-MSE) should be obtained by IN1; this expectation is confirmed by Table 2 and figure 4. Table 2 and figure 5 show when the data are generated under model 0 (the most unfavorable conditions for IN1), the performances of both predictors are approximately the same, although predictor IN0 gets slightly better results.

We conclude that the variance parameters of the random slopes and/or the correlation parameter between the two play an important role in obtaining model performance. In this simulation study, IN1 performs well even when the underlying true conditions are not fully favorable. These results are consistent with the theory in the literature that frames random slope mixed models as a more flexible alternative to mixed models with random intercept only. In practice, after establishing the appropriateness of including random slopes in the predictons, more analysis is needed to determine the most optimal parameterization of the employed ARRCP model. See section E.3 in the supplementary data online for simulation that compares plug-in predictors for an example of such analyses.

5.3 Simulation 3

Simulation 3 studies the behavior of the parametric bootstrap estimator of the MSE of a predictor $\hat{p}_{ij}$ of p_{ij}. More concretely, we use three different bootstrap estimators to obtain MSEs with the IN1 predictors. Specifically, we consider a parametric bootstrap approximation without a bias correction (PB) and two double bootstrap procedures, the Hall and Maiti (2006) bias-corrected bootstrap (HM) and the Erciulescu and Fuller (2013) bias-corrected bootstrap (EF). See appendix C of the supplementary data online for more information on the considered bootstrap estimators. Performance is assessed relative to the empirical (true) MSE obtained from Simulation 1, where $MSE_{ij}^{\text{in}} = \left(RMSE_{ij}^{\text{in}}\right)^2$.

Table 2. Performance Measures for Plug-In Predictors under Model 1 and Model 0 (Simulation 2). The data in columns 2 and 3 are generated with model 1 (random intercepts and slopes), whereas the data in columns 4 and 5 are generated with model 0 (random intercepts only).

	Model 1		Model 0	
	IN1	IN0	IN1	IN0
10^3 ABIAS	0.6805	0.9964	0.9526	0.9760
10^3 RMSE	23.2990	27.1146	25.7758	25.7204
ARBIAS	0.3005	0.4518	0.4385	0.4508
RRMSE	10.4265	12.2292	11.8440	11.8163

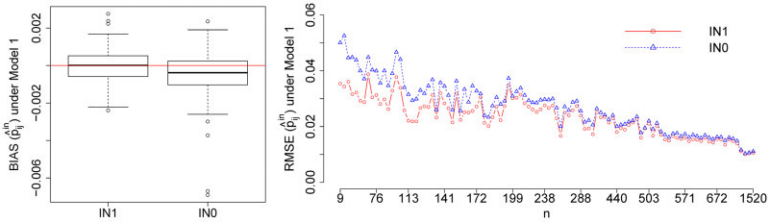

Figure 4. BIAS and RMSE of Plug-In Predictors under Model 1 (Simulation 2).

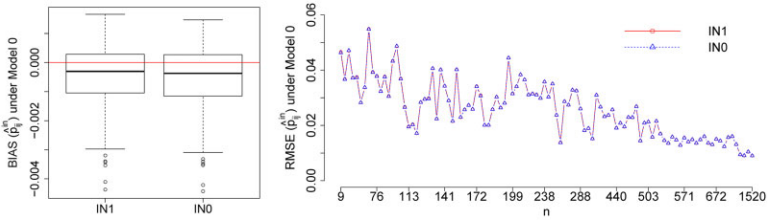

Figure 5. BIAS and RMSE of Plug-In Predictors under Model 0 (Simulation 2).

The simulation procedure was as follows:

(1) Repeat steps 1.1 through 1.3 independently, $R = 500$ times ($r = 1, \ldots, R$)
  1.1 Generate a sample $(y_{ij}^{(r)}, x_{ij})$, $i \in \mathbb{I}$, $j \in \mathbb{J}$ in the same way as in simulation 1.
  1.2 Calculate the estimators $\hat{\beta}_1^{(r)}$, $\hat{\beta}_2^{(r)}$, $\hat{\beta}_3^{(r)}$, $\hat{\beta}_4^{(r)}$ $\hat{\beta}_5^{(r)}$, $\hat{\sigma}^{(r)}$, $\hat{\phi}_2^{(r)}$, $\hat{\phi}_5^{(r)}$, $\hat{\rho}_{25}^{(r)}$.
  1.3 Calculate $\text{mse}_{ij}^{*(r)} \in \{\text{mse}^{*\text{PB}}(\hat{p}_{ij}^{\text{in}}), \text{mse}^{*\text{HM}}(\hat{p}_{ij}^{\text{in}}), \text{mse}^{*\text{EF}}(\hat{p}_{ij}^{\text{in}})\}$.
(2) For each bootstrap estimator*, calculate

  Bias (within): $BI_{ij}^{*} = \frac{1}{R}\sum_{r=1}^{R}\left(\widehat{MSE}_{ij}^{*(r)} - MSE_{ij}^{\text{in}}\right)$

Table 3. Comparative Performance of mse* $(\hat{p}_{ij}^{\text{in}})$ estimators for $B_1 = 500$

	AB	(x10^3)	RE	(x10^3)	ARB (%)	RRE (%)	Time
PB	0.0398		0.1329		6.1007	21.7383	3.5613 min
HM	0.0249		0.1489		4.1405	24.8549	11.0111 min
EF	0.0217		0.1579		3.8079	26.3079	7.4624 min

Absolute Bias: $AB^* = \frac{1}{IJ}\sum_{i=1}^{I}\sum_{j=1}^{J}\left|BI_{ij}^*\right|$

Root-MSE (within): $RE_{ij}^* = \left[\frac{1}{R}\sum_{r=1}^{R}\left(\widehat{MSE}_{ij}^{*(r)} - MSE_{ij}^{\text{in}}\right)^2\right]^{1/2}$

Root-MSE: $RE^* = \frac{1}{IJ}\sum_{i=1}^{I}\sum_{j=1}^{J} RE_{ij}^*$

(3) Calculate the corresponding relative performance measures (in percent).

Relative Bias (within): $RB_{ij}^* = 100\left(\frac{BI_{ij}^*}{MSE_{ij}^{\text{in}}}\right)$

Relative RMSE (within): $RRE_{ij}^* = 100 \times \left(\frac{RE_{ij}^*}{MSE_{ij}^{\text{in}}}\right)$

Absolute Relative Bias: $ARB^* = \frac{1}{IJ}\sum_{i=1}^{I}\sum_{j=1}^{J}\left|RB_{ij}^*\right|$

Relative Root-MSE: $RRE^* = \frac{1}{IJ}\sum_{i=1}^{I}\sum_{j=1}^{J} RRE_{ij}^*$

See appendix C of the supplementary data online for details on the implemented simulation study and for more information on algorithms and appropriate modifications.

In this simulation we used $B_1 = 500$ replicates in the first level, as all considered procedures converged with this number of iterations. For the two double bootstrap approaches (HM and EF), we take $B_2 = 2$ and $B_2 = 1$ replicates, respectively.

Table 3 shows the performance measures and computational times required. As expected, corrected bootstrap estimators (HM and EF) have lower relative and absolute biases than their uncorrected counterpart (PB). However, consistent with this decrease in bias, the RE increases with the bias corrections. Nevertheless, the improvement in bias compensates for the corresponding increases in variance. Both bias corrected bootstraps have comparable performance, with the EF correction showing a slight edge in term of bias and having the added advantage of greater speed, with runtimes more comparable to the uncorrected PB.

Since the performance measures presented in Table 1 are averaged over the 500 bootstrap samples, it is worth examining the distribution of the relative biases and relative root-MSEs. Figure 6 presents boxplots of these measures for the three considered bootstrap methods. The large reduction in bias with the HM and EF bootstrap estimators offsets the corresponding observed increases in the RRE_{ij}.

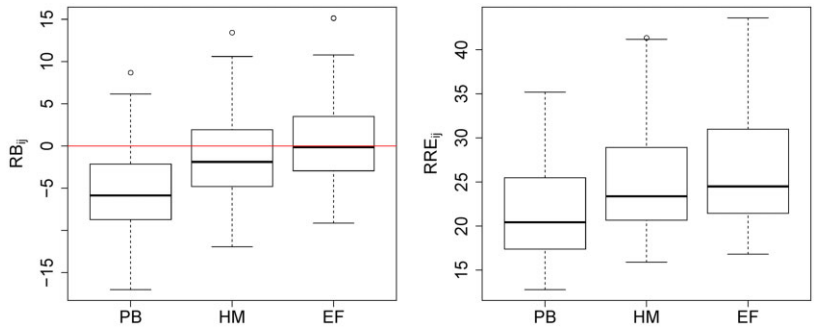

Figure 6. RB and RRE of Each $\text{mse}^*\left(\hat{p}_{ij}^{\text{in}}\right)$ with $B_1 = 500$ and $B_2 = 2$ (HM) or $B_2 = 1$ (EF).

Given its substantive bias correction, trivial variance increase, and relatively low computation requirements, we selected the EF method for the application presented in section 6, employing a B_1 equal to or greater than 500 and a $B_2 = 1$. We note that all three approximations presented have optimal properties for estimating the RMSE of poverty proportions.

6. APPLICATION TO REAL DATA

For the real data application, we utilize the following the ARRCP model (see (1)): y_{ij} is the sample count of people below the poverty threshold in province i and sex j (the dependent variable), $v_{ij} = n_{ij}$ is the sample size, $x_{1,ij}$ is the intercept and $x_{2,ij}$, $x_{3,ij}$, $x_{4,ij}$, and $x_{5,ij}$ are the values of age3, edu1, cit1, and lab2, respectively, defined in section 2. The selected model contains only two random slopes for $x_{2,ij}$ and $x_{5,ij}$, so that the corresponding model parameters and random effects are ϕ_2, ϕ_5, ρ_{25}, and $u_{ij} \sim N(0,1)$, $(v_{2,k}, v_{5,k})' \sim N_2(\mathbf{0}, \boldsymbol{V}_{25})$, $\mathbf{0} = (0,0)'$, and $\boldsymbol{V}_{25}(\rho_{25}) = \begin{pmatrix} 1 & \rho_{25} \\ \rho_{25} & 1 \end{pmatrix}$. The natural parameter is

$$\eta_{ij} = \log \mu_{ij} = \log n_{ij} + \sum_{\ell=1}^{5} \beta_\ell x_{\ell,ij} + \sigma u_{ij} + \phi_2 v_{2,k(i)} x_{2,ij} + \phi_5 v_{5,k(i)} x_{5,ij},$$

and the selected model has a cAIC of 744.71 (d.f. = 48.33, conditional loglikelihood = −324.02). Candidate models with small cAIC were evaluated based on the following criteria: (1) social-economic interpretability and statistical significance of fitted regression parameters, (2) nonzero variance parameters of random effects, (3) convergence of the ML-Laplace approximation algorithm, and (4) validity of model assumptions. For more information on model selection in SAE, see Vaida and Blanchard (2005) and Lombardía et al. (2017)

Table 4. Regression Parameter Estimates and Basic Percentile Confidence Intervals ($\alpha = 5$ Percent), for the ARRCP Model Used in the SLCS SAE Real Data Application.

	β_1	β_2	β_3	β_4	β_5	σ	ϕ_2	ϕ_5	ρ_{25}
2.5%	−2.0939	−8.4242	0.1903	−2.1321	3.6580	0.1102	0.9589	0.4625	−1.0000
Estimate	−1.3806	−4.2120	1.0048	−1.3491	6.9135	0.1414	2.0617	2.5985	−0.9432
97.5%	−0.6107	−0.2015	1.8523	−0.5056	10.3916	0.1901	3.8284	5.0808	−0.8864

among others. Appendix A in the supplementary data online provides details on the model selection process.

Table 4 presents the regression parameter estimates and the basic percentile confidence intervals at $\alpha = 5$ percent discussed later in this section. The estimated regression parameters can be interpreted from a socio-economic perspective. A higher percentage of unemployed (lab2) or less educated (edu1) population is positively associated with poverty, whereas higher proportions of late-career population (age3) or foreign citizens (cit1) are associated with reduced poverty rates: see Molina and Rao (2010), Esteban et al. (2012), Molina et al. (2014), Morales et al. (2015), Benavent and Morales (2016), Boubeta et al. (2016), and Marhuenda et al. (2017). In the paragraphs below, the socio-economic interpretation of the realized model parameters is discussed in more detail.

As the population ages, employment tends to be characterized by job stability and higher income (reduced poverty risk), as reflected latest INE statistics. In 2020, population between 45 to 64 years old had the highest average household income (for both men and women), followed by the population aged 65 and above. This trend corresponds to the 2008 pattern presented in INE (2020a). This poverty *reduction* effect of is reflected by the $\hat{\beta}_2$ value of −4.2120.

Higher levels of attained education are associated with better job opportunities and salaries; conversely, lower levels of attained education are associated with increased poverty risk. In the 2020 SLCS, people with incomplete preschool, primary, and/or secondary education have the highest percentage of relative poverty risk (28.7 percent), compared to people with completed secondary education (18.6 percent in the edu2 category) and people with tertiary education (9.1 percent in the edu3 category). This is pattern is quite like that in 2008 SLCS case study data, which has 21.2 percent of the population at risk of poverty for edu1, 12.9 percent for edu2, and 7.0 percent for edu3; see INE (2020d). Recall that $x_{3,ij}$ in our ARRCP model represents the ed1 category (illiterate, with complete or incomplete primary education or with incomplete secondary education). Consistent with the expected *increase* in poverty associated with this low education attainment category, $\hat{\beta}_3$ is 1.0048.

A higher percentage of foreign citizens in the population tends be associated with a reduction in poverty, possible because people move to the Spanish provinces that offer greater employment opportunities. The province with the highest number of foreigners in 2008 was Madrid, followed by Barcelona, which is the province with the highest income group ($k = 5$); see INE (2020c). The poverty *reduction* effect is reflected by the $\hat{\beta}_4$value of -1.3491.

Finally, higher percentage of unemployed persons is associated with increases in poverty, or alternatively, a high percentage of labor activity is a key factor in minimizing the risk of exclusion and poverty. In the 2008 SLFSS data, the highest unemployment rates are in the Andalucia and Extremadura provinces, which are classified into the income group classes with the lowest mean average income; see INE (2020b). Consistent with the expected increase in poverty associated with high percentages of unemployed persons, $\hat{\beta}_5$ is 6.9135.

After establishing their consistent socio-economic interpretations, the significance of the fixed and random effects parameters' is assessed by computing confidence intervals. For this, we use basic percentile method to obtain a $(1-\alpha)\%$ bootstrap confidence interval for our parameter vector; see appendix D in the supplementary data online for more information. Following the guidelines given by Davison and Hinkley (1997), we used 999 bootstrap replicates to attain a 95 percent confidence level. None of the confidence interval provided in Table 4 contain zero, providing support for the inclusion of the random coefficients in the ARRCP model. Notice that the widest intervals are associated with β_2 and β_5 and ϕ_2 and ϕ_5, which may further support the important contribution of the random coefficients to the variance of the ARRCP model.

The last step of the ARRCP model validation/assessment procedure is to assess goodness of fit. For this, we calculated, the Pearson residuals of the model as: $r_{ij} = \frac{\mu_{ij} - \hat{\mu}_{ij}}{\sqrt{\hat{\mu}_{ij}}}, \quad i \in \mathbb{I}, j \in \mathbb{J}.$

Figure 7 plots the residuals against the predicted poverty values (left) and plots the predicted values against the observed poverty values (right). The residuals are randomly centered around the line $y = 0$, with the majority of values falling between 1 and -1, without responding to any particular pattern. However, there are 7 residuals around the -2 range; see table 5.

All seven residuals have large negative values. In the studied data, these domains have the lowest proportion of poverty and the highest average income, with one exception. Residual 85 (position 20) belongs to the $k = 3$ income group, but also has a small number of poor people. That said, its modeled values appear to provide a good fit to the actual counts as shown in figure 7. See section F.2. in the supplementary data online for more details on the model validation process, particularly with respect to the assessment of random effects.

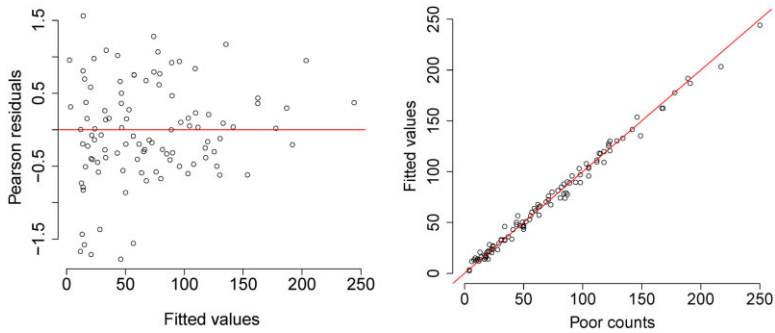

Figure 7. Goodness of Fit of the ARRCP Model.

Table 5. Descriptive of the Highlighted Seven Residuals (Outliers)

d	k	Province	Sex	r_{ij}	n_{ij}	y_{ij}	p_{ij}
61	5	Navarra	1	−1.7754	571	34	0.0595
33	5	Gerona	1	−1.7111	178	13	0.0730
87	4	Teruel	1	−1.6684	82	6	0.0732
23	5	Castellón	1	−1.5768	129	9	0.0698
62	5	Navarra	2	−1.5577	633	45	0.0711
88	4	Teruel	2	−1.4340	81	8	0.0988
85	3	Tarragona	1	−1.3666	162	21	0.1296

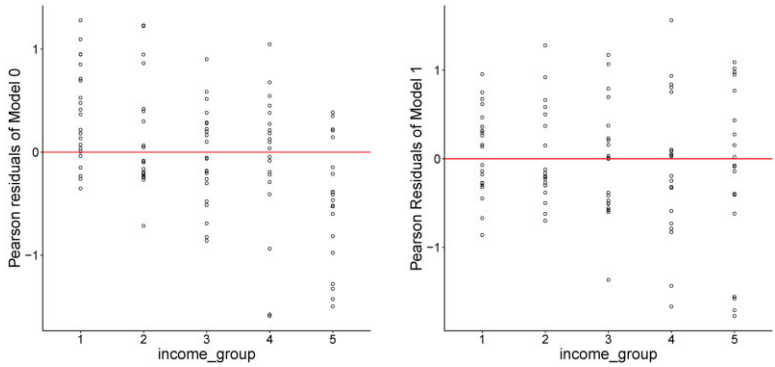

Figure 8. Distribution of Pearson Residuals by Income Group $k, k=1, \cdots, 5$.

To assess the improvements in the model by including random coefficients, figure 8 plots the Pearson residuals of model 0 (random intercept) and model 1 (random intercept and random slopes) against the five income groups. Including the random coefficients in the model improves the model fit,

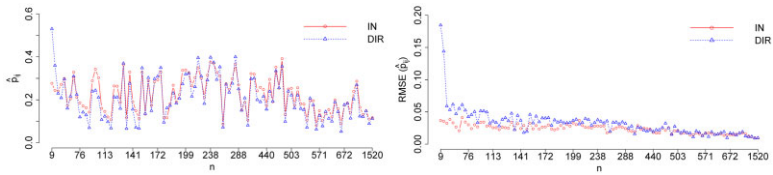

Figure 9. Poverty Proportions Estimates $\hat{p}_{ij}$ and Associated RMSE$_{ij}$, Ordered by Sample Size. Modeled estimates are represented as IN; direct estimates are represented as DIR.

especially in the $k = 1$, $k = 2$, and $k = 5$ income group clusters. Having validated the model on all stated criteria, we use it to obtain plug-in predictions from the SLCS data file to obtain the poverty proportion estimates and associated RMSE$_{ij}$.

Figure 9 (left) plots the plug-in predictions (SAE) and the classic Hájek estimates (direct estimates) of the poverty proportions. Figure 9 (right) gives the estimates of the model-based and design-based root MSEs, respectively. In the case of the plug-in predictors, the parametric bootstrap incorporated the EF bias correction with $B_1 = 500$ and $B_2 = 1$ replications.

Figure 9 (left) demonstrates the divergence of the direct estimator and the plug-in predictors diverge for domains with smaller sample sizes, as the direct p_{ij} estimates are considerably larger than their plug-in counterparts. Both sets of estimates converge as the domain sample size increases. This trend is consistent with the estimated root MSEs plotted in figure 9 (right). With the plug-in predictor, the estimated root MSEs decrease smoothly as sample size increases. The root MSEs for the direct estimates are considerably larger and more variable, with large peaks especially near the origin. The corresponding sets of root MSEs converge as the sample size increases.

Delving a bit deeper, we examine the domain-level RRMSE$_{ij}$'s for the smallest and largest domains, respectively. The largest direct-estimate RRMSE$_{ij}$ (19.2340 percent) corresponds to the male population in Soria (domain 83). The corresponding plug-in prediction is less than five percent. The largest direct estimate RRMSE$_{ij}$ (5.0311 percent) corresponds to the female population in Barcelona (domain 16). The corresponding plug-in prediction is nearly equivalent.

As mentioned in the introduction, poverty proportion maps are a widely used tool to inform socio-political actors, who use them to develop necessary system reforms. Figure 10 shows two maps. On the right, the five different shades distinguish between estimated poverty proportion ranges. On the left, the five different shades distinguish between the income group categories.

In general, there is strong correspondence between income group and poverty proportion, with some minor differences. For example, in the Cadiz, Salamanca, Soria, Lerida, Santa Cruz de Tenerife, and Las Palmas regions, the

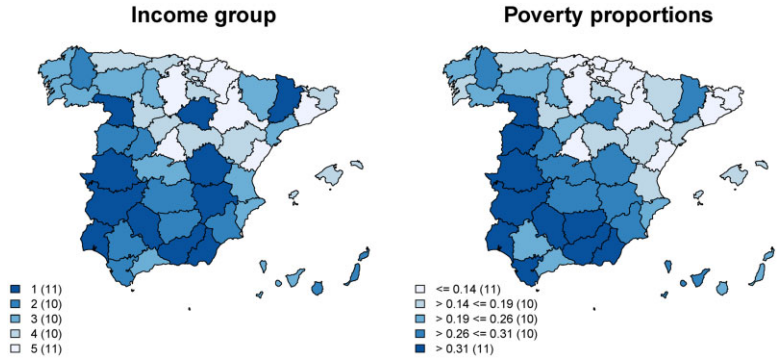

Figure 10. Estimated Poverty Proportions in Spanish Provinces by Income Group.

income groups change slightly, increasing from $k = 1$ to $k = 2$. Lérida is of particular interest. Usting the 2008 SLCS data, Lérida is classified in income group cluster, $k = 1$ (the lowest average income per household unit). However, its surrounding areas are characterized as high-income groups, such as Barcelona. Indeed, the substantively lower income category or Lerida compared to the other provinces of Cataluna is present in the most recent data release from Spanish Tax Agency, which provides gross and average income by Autonomous Community. The ARRCP prediction for this province still distinguishes it from its neighbors. The same results were obtained by Molina and Rao (2010) which utilized a nested error regression model.

The analysis for Lerida exemplifies the utility of poverty maps. It is reasonable to assume that areas within the same province will have similar economic structures. This example contradicts this assumption, offering insight into ineffective policies that could result from a generalist localization of funds. Broadening the focus to all the provinces, we can draw several conclusions. First, the situation in Spain is alarming to say the least, as more than 40 percent of the provinces are located in the groups with the highest proportion of predicted poverty. However, predicted poverty is not equally distributed across Spain. There are clear patterns. The provinces with the highest poverty ratios are located in the southern and western fringe of the Peninsula, with a total of 11 provinces with a poverty ratio value above 0.31: Zamora, Salamanca, Cáceres, Badajoz, Huelva, Cádiz, Córdoba, Jaén, Granada, Almería, Ceuta, and Melilla. At the opposite end, the provinces with the lowest proportion of the population below the poverty line are Cantabria, Vizcaya, Guipúzcoa, Álava, Burgos, Zaragoza, Gerona, Barcelona, Castellón, and Madrid. Molina and Rao (2010) and Boubeta et al. (2017) obtained similar results using the 2008 SLCS data.

This coincidence in itself is informative, since the studies are carried out with different years of the SLCS. However, the same divergent pattern appears

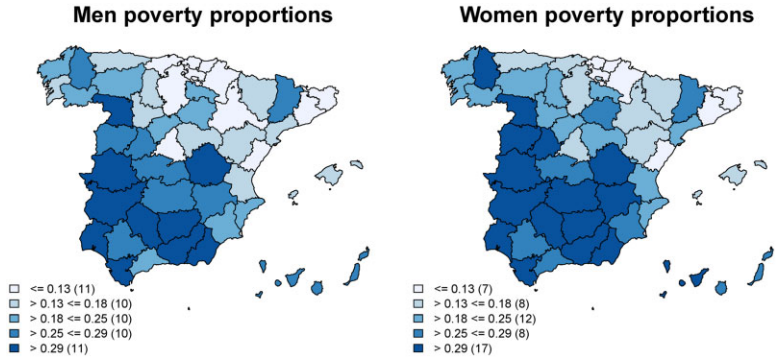

Figure 11. Estimated Poverty Proportions in Spanish Provinces by Sex.

in all these studies: the northeaster provinces have a lower proportion of poverty than the south-western provinces, i.e., the "Two Spains." Tirado et al. (2016) point out the transcendental importance in these patterns, with this systematic divergence established and stabilized since 1930. Thus, general policies do not seem to have led to a reversal of the trend. The authors highlight important inherent underlying differences, pointing out that the high economic power of the provinces in the northeast of the Peninsula may be associated with the importance of proximity to European markets, boosting the development of the regions employed there. This is an important fact because the relative poverty of the provinces in the south and west of Spain is substantially higher than the remaining regions in Spain, with especially pronounced differences in recent years. To start to alleviate these imbalances, it is essential to design policies that take into account the specific characteristics of each region.

Finally, we carry out a gender gap analysis. Figure 11 shows the poverty distribution map by sex. The gender gap is clear. Both maps show the same trend as figure 10, that is, in the northern and eastern fringe there are lower proportions of poverty than in the southern and central regions of the Peninsula.

However, there are clear differences in poverty mapping by gender. First, corresponding poverty ratios exhibit consistently higher poverty ratios for women than men. Moreover, there are fewer providences in the lowest poverty ratio category for women than for men.

The highest proportion of poverty among men is especially located in the south, specifically in Ceuta, Almería, Granada, Jaén, Córdoba, Cádiz, and Huelva, as well as in regions toward the west, such as Cáceres and Badajoz. Further to the north and to the center, there are isolated cases, corresponding to Zamora and Cuenca respectively.

For women, the dark blue color expands visibly, with a higher proportion of poverty in the central and northern provinces, and also at the level of Santa

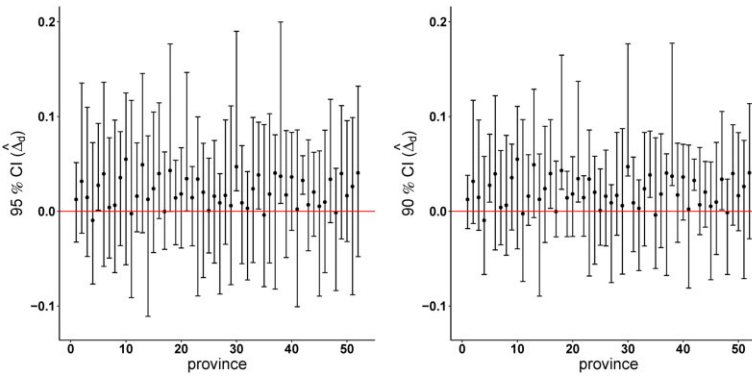

Figure 12. Basic Percentile Bootstrap Confidence Intervals at 95 and 90 percent for $\hat{\Delta}_d$.

Cruz de Tenerife. These results are consistent with Molina and Rao (2010) or Boubeta et al. (2017) are likewise internally consistent with our stated expectations for the prediction model.

To complete the gender inequality analysis, we developed confidence intervals to test whether visual differences are statistically significant. Let $\hat{\Delta}_d = \hat{p}_{i2} - \hat{p}_{i1}$ be the difference in poverty proportions for women ($\hat{p}_{i2}$) relative to men ($\hat{p}_{i1}$), with percentile confidence intervals calculated using a parametric bootstrap algorithm (see appendix D in the supplementary data online). Figure 12 presents the basic bootstrap percentile confidence intervals at 95 percent (left) and 90 percent (right) confidence levels, respectively.

Although the poverty proportions are greater for women than for men, at the 95 percent confidence level, only six of these differences are statistically significant: (from north to south) Palencia, Soria and Ávila (Castilla y León), Murcia (Región de Murcia), Huelva (Andalucía), and Santa Cruz de Tenerife (Islas Canarias).

These results are consistent with those in figure 11. With the exception of Huelva, the proportion of women in poverty increases within the same provinces. Furthermore, these identified provinces are all in low income groups, with the maximum of $k = 3$; see figure 10. In summary, we observe significant differences between corresponding male and female poverty ratios in the southwest, a geographic area characterized by higher poverty ratios and lower average income categories. If we decrease the confidence level to 90 percent, significant differences are also detected in Valladolid (Castilla León), Cuenca (Castilla la Mancha), and Granada (Andalucía), all of which display the same pattern except Valladolid, which is in a higher income group category ($k = 4$).

Our results are consistent with other studies. For example, Molina et al. (2014) presented 95 percent highest posterior density intervals by gender and Spanish province in a study using data from the 2006 ES SILC.

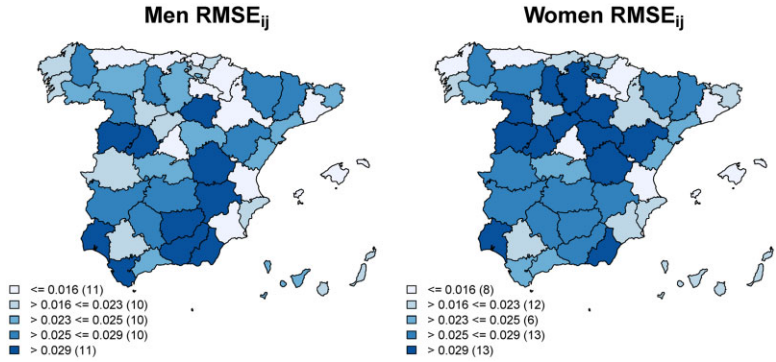

Figure 13. Spatial Distribution of Estimated RMSE$_{ij}$ in Spanish Provinces by Sex.

The evident differences in women's living conditions compared to men's are the product of a complex reality that is not fully captured by poverty ratio indicators. Further research is needed to develop other indicators that provide a more complete picture of inequality and its location to make further progress in narrowing the gender gap.

Finally, figure 13 shows the RMSE$_{ij}$ of the poverty proportion estimates plotted in figure 11. The poverty ratios with the highest values of RMSE$_{ij}$ are concentrated in regions of Castilla y León and in southern regions, specifically in Andalucía provinces, as well as Lerida, whose special features are discussed above.

In general, the RRMSE$_{ij}$ of the women's poverty ratios tend to be higher than for the male poverty ratios in the same geography. However, there are exceptions; for example, La Coruna.

Figure 14 maps sample size by province for men and women, respectively. Examining figures 13 and 14 together, a clear pattern emerges: the larger the sample sizes, the lower the RMSE$_{ij}$. Thus, this explains the anomaly of La Coruna. This analysis is consistent with the results presented earlier in figure 9.

Ultimately, there is no reason to restrict our investigation to poverty ratios. The poverty predictor allows us to detect multiple patterns, but has limitations. For example, not all provinces share same cost of living but all are assessed with respect to the same poverty threshold. This does not detract from our findings. It should pique interest expanding this, or other research, to different indicators. Likewise, as proposed by Reluga et al. (2023), the analysis of simultaneous confidence intervals to detect the existence of significant differences between provinces could be of interest for fund distribution policies.

7. CONCLUSIONS

Poisson GLMMs have gained popularity in the SAE literature in recent years due to their relative simplicity and incorporation of inter-area heterogeneity.

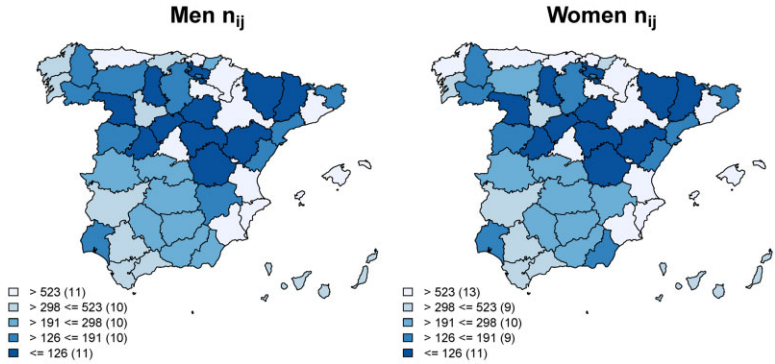

Figure 14. Spatial Distribution of Sample Size in Spanish Provinces by Sex.

However, statistical inference in mixed models with exclusively fixed regression coefficients can by excessively rigid when the relationship between dependent and independent variables varies by domain, as in the case study presented here. This article analyses the poverty ratio in Spain in 104 domains corresponding to the crossing of the 52 Spanish provinces (including the cities of Ceuta and Melilla) and the two sexes, employing an original area-level random regression coefficient Poisson model (ARRCP model).

Our ARRCP model includes random effects for two variables, with slopes differing by income group category. We obtain ML estimators of the model parameters, with mode predictors of the random effects calculated by a Laplace approximation algorithm. After defining two theoretical predictors (SP and BP) and associated empirical version (ESP and EBP), we carry out comprehensive simulation studies to assess their statistical properties, in particular with respect to the case study data. Here, the EPB generally yielded smaller RMSE and was less computationally intensive, although we believe that the ESP should be considered in other applications, given the strength of its results in our simulations. However, the computationally simpler plug-in predictor – by definition biased – exhibited smaller bias than the EPB in our simulations, with similar estimated levels of bias to the BP and smoother estimates. For these reasons, we selected the plug-in predictor for our study.

We considered three different parametric bootstrap estimators of MSE for the plug-in predictor: one that does not apply a bias correction and two bias-corrected estimators based on the definition of a double bootstrap. Our simulation studies verified the effectiveness of the bias corrections, which reduced bias at the cost of an acceptable increase in the RMSE with little additional computational burden. In our case study, we utilize the EF bias correction, which was practically unbiased and provided an acceptable RMSE estimate but is the computationally faster method of the two considered bias-corrected bootstraps.

We applied our ARRCP model to real data, applied to the 2008 SLCS and SLFS data, using our recommended plug-in predictor to estimate the poverty proportions in 104 domains In comparing domain-level relative root MSE of our SAE predictions to corresponding (direct) Hajek-type estimates, we found that plug-in estimator had consistently better performance. Finally, we present our predicted poverty ratios represented in a poverty map, which shows a clear north-south and east-west pattern of increasing poverty rates in Spain, with generally higher rates for women.

Supplementary Materials

Supplementary materials are available online at academic.oup.com/jssam.

REFERENCES

Benavent, R., and Morales, D. (2016), "Multivariate Fay-Herriot Models for Small Area Estimation," *Computational Statistics and Data Analysis*, 94, 372–390.

———. (2021), "Small Area Estimation under a Temporal Bivariate Area-Level Linear Mixed Model with Independent Time Effects," *Statistical Methods and Applications*, 30, 195–222.

Berg, E. J., and Fuller, W. A. (2014), "Small Area Prediction of Proportions with Applications to the Canadian Labour Force Survey," *Journal of Survey Statistics and Methodology*, 2, 227–256.

Boubeta, M., Lombardía, M. J., and Morales, D. (2016), "Empirical Best Prediction under Area-Level Poisson Mixed Models," *TEST*, 25, 548–569.

———. (2017), "Poisson Mixed Models for Studying the Poverty in Small Areas," *Computational Statistics and Data Analysis*, 107, 32–47.

Chambers, R., Salvati, N., and Tzavidis, N. (2016), "Semiparametric Small Area Estimation for Binary Outcomes with Application to Unemployment Estimation for Local Authorities in the UK," *Journal of the Royal Statistical Society: Series A*, 179, 453–479.

Chandra, H., Chambers, R., and Salvati, N. (2019), "Small Area Estimation of Survey Weighted Counts under Aggregated Level Spatial Model," *Survey Methodology*, 45, 31–59.

Chandra, H., Salvati, N., and Chambers, R. (2017), "Small Area Prediction of Counts under a Non-Stationary Spatial Model," *Spatial Statistics*, 20, 30–56.

Chen, S., and Lahiri, P. (2012), "Inferences on Small Area Proportions," *Journal of the Indian Society of Agricultural Statistics*, 66, 121–124.

Davison, A. C., and Hinkley, D. V. (1997), *Bootstrap Methods and Their Application*, Cambridge: Cambridge University Press.

Demidenko, E. (2013), *Mixed Models: Theory and Applications with R* (2nd ed.), Hoboken: John Wiley and Sons.

Dempster, A. P., Rubin, D. B., and Tsutakawa, R. K. (1981), "Estimation in Covariance Components Models," *Journal of the American Statistical Association*, 76, 341–353.

Erciulescu, A. L., and Fuller, W. A. (2013), "Small area prediction of the mean of a binomial random variable," in Joint Statistical Meeting 2013 Proceedings—Survey Research Methods Section, Session 37 Small-Area Estimation: Theory and Applications, Montréal, CA: American Statistical Association, pp. 855–863. Available at: http://www.asasrms.org/Proceedings/y2013f.html.

EstebanM. D.LombardíaM. J.López-VizcaínoE.MoralesD.PérezA. (2020), "Small Area Estimation of Proportions under Area-Level, Compositional Mixed Models," *TEST*, 29, 793–818.

Esteban, M. D., Morales, D., Pérez, A., and Santamaría, L. (2012), "Small Area Estimation of Poverty Proportions under Area-Level Time Models," *Computational Statistics and Data Analysis*, 56, 2840–2855.

Franco, C., Bell, W. R. (2022), "Using American Community Survey Data to Improve Estimates from Smaller US Surveys through Bivariate Small Area Estimation Models," *Journal of Survey Statistics and Methodology*, 10, 225–247.

Ghosh, M., Kim, and D., SinhaK.Maiti, T., and Katzoff, M., Parsons, V. L. (2009), "Hierarchical and Empirical Bayes Small Domain Estimation and Proportion of Persons without Health Insurance for Minority Subpopulations," *Survey Methodology*, 35, 53–66.

Hall, P., Maiti, T. (2006), "On Parametric Bootstrap Methods for Small Area Prediction," *Journal of the Royal Statistical Society: Series B (Statistical Methodology)*, 68, 221–238.

Hobza, T., Morales, D. (2013), "Small Area Estimation under Random Regression Coefficient Models," *Journal of Statistical Computation and Simulation*, 83, 2160–2177.

Hobza, T., and Morales, D. (2016), "Empirical Best Prediction under Unit-Level, and Logit Mixed Models," *Journal of Official Statistics*, 32, 661–692.

Hobza, T., Morales, and D., Santamaría, L. (2018), "Small Area Estimation of Poverty Proportions under and Unit-Level, Temporal Binomial-Logit Mixed Models," *TEST*, 27, 270–294.

INE (2020a), "Average per Person and Consumption Unit by Age and Sex." Available at: https://, www., ine., es/, and jaxiT3/, Tabla.htm?t=9942&L=1 (accessed June 2022).

INE (2020b), "Economic Activity, Unemployment and Employment Rates, by Province." Available at: https://www.ine.es/jaxiT3/Tabla.htm?t=3996&L=1 (accessed June 2022).

INE (2020c), "Main Series of Population since 1998." Available at: https://www.ine.es/dynt3/ine-base/en/index.htm?path=/t20/e245/p08/ (accessed June 2022).

INE (2020d), "Wages, Income, Social Cohesion." Available at: https://www.ine.es/jaxiT3/Datos.htm?t=11025 (accessed June 2022).

INE (2022), "Living Condition Survey (LCS)." Available at: https://www.ine.es/dynt3/metadatos/en/RespuestaDatos.htm?oe=30453 (accessed June 2022).

LiuB.LahiriP. (2017), "Adaptive Hierarchical Bayes Estimation of Small Area Proportions," *Calcutta Statistical Association Bulletin*, 69, 150–164.

LombardíaM. J.López-VizcaínoE.RuedaC. (2017), "Mixed Generalized Akaike Information Criterion for Small Area Models," *Journal of the Royal Statistical Society: Series A (Statistics in Society)*, 180, 1229–1252.

López-VizcaínoE., Lombardía, and M. J., Morales, D. (2013), "Multinomial-Based Small Area Estimation of Labour Force Indicators," *Statistical Modelling*, 13, 153–178.

López-Vizcaíno, E., Lombardía, and M. J., Morales, D. (2015), "Small Area Estimation of Labour Force Indicators under a Multinomial Model with Correlated Time and Area Effects," *Journal of the Royal Statistical Society: Series A (Statistics in Society)*, 178, 535–565.

Marhuenda, Y., Molina, and I., Morales, D. (2013), "Small Area Estimation with Spatio-Temporal, Fay-Herriot Models," *Computational Statistics and Data Analysis*, 58, 308–325.

Marhuenda, and Y., Molina, I., Morales, D., and Rao, J. N. K. (2017), "Poverty Mapping in Small Areas under a Twofold Nested Error Regression Model," *Journal of the Royal Statistical Society: Series A (Statistics in Society)*, 180, 1111–1136.

MarhuendaY.Morales, D., Pardo, M. C. (2014), "Information Criteria for Fay-Herriot, Model Selection," *Computational Statistics and Data Analysis*, 70, 268–280.

Matuschek, and H., Kliegl, R., Vasishth, S., and Baayen, H.BatesD. (2017), "Balancing Type I Error and Power in Linear Mixed Models," *Journal of Memory and Language*, 94, 305–315.

Militino, A. F., Ugarte, M. D., Goicoa, T. (2015), "Deriving Small Area Estimates from Information Technology Business Surveys," *Journal of the Royal Statistical Society: Series A (Statistics in Society)*, 178, 1051–1067.

Molina, I., Nandram, and B., Rao, J. N. K. (2014), "Small Area Estimation of General Parameters with Application to Poverty Indicators: A Hierarchical Bayes Approach," *The Annals of Applied Statistics*, 8, 852–885.

Molina, I., Rao, and J. N. K. (2010), "Small Area Estimation of Poverty Indicators," *The Canadian Journal of Statistics*, 38, 369–385.

Molina, I., Saei, A., Lombardía, and M. J. (2007), "Small Area Estimates of Labour Force Participation under Multinomial Logit Mixed Model," *Journal of the Royal Statistical Society: Series A (Statistics in Society)*, 170, 975–1000.

Morales, D., Esteban, and M. D., Pérez, A., Hobza, T. (2021), *A Course on Small Area Estimation and Mixed Models. Methods, Theory and Applications in R*, Switzerland: Springer.

Morales, and D., Krause, J., Burgard, J. P. (2022), "On the Use of Aggregate Survey Data for Estimating Regional Major Depressive Disorder Prevalence," *Psychometrika*, 87, 344–368.

Morales, D., Pagliarella, and M. C., Salvatore, R. (2015), "Small Area Estimation of Poverty Indicators under Partitioned Area-Level, Time Models," *SORT-Statistics and Operations Research Transactions*, 39, 19–34.

Moura, and F. A. S., Holt, D. (1999), "Small Area Estimation Using Multilevel Models," *Survey Methodology*, 25, 73–80.

Prasad, N. G. N., Rao, and J. N. K. (1990), "The Estimation of the Mean Squared Error of Small-Area Estimators," *Journal of the American Statistical Association*, 85, 163–171.

RaoJ. N. K., Molina, and I. (2015), *Small Area Estimation* (2nd ed.), Hoboken: Wiley.

Reluga, K., Lombardía, and M. J., SperlichS. (2023), "Simultaneous Inference for Empirical Best Predictors with a Poverty Study in Small Areas," *Journal of the American Statistical Association*, 118, 583–595.

SwamyP. A. (1970), "Efficient Inference in a Random Coefficient Regression Model," *Econometrica: Journal of the Econometric Society*, 38, 311–323.

Tirado, D. A., and Díez-Minguela, A., Martinez-Galarraga, J. (2016), "Regional Inequality and Economic Development in Spain, 1860-2010," *Journal of Historical Geography*, 54, 87–98.

Tzavidis, N., and Ranalli, M. G., Salvati, N., Dreassi, E., and Chambers, R. (2015), "Robust Small Area Prediction for Counts," *Statistical Methods in Medical Research*, 24, 373–395.

United Nations (2022), "Peace, Dignity and Equality on a Healthy Planet." Available at: https://, www., un., org/, en/, global-, issues/, ending-, and poverty (accessed August 2022).

Vaida, F.BlanchardS. (2005), "Conditional Akaike Information for Mixed-Effect Models," *Biometrika*, 92, 351–370.

WangX.BergE. J.Zhu, Z., and Sun, D.DemuthG. (2018), "Small Area Estimation of Proportions with Constraint for National Resources Inventory Survey," *Journal of Agricultural, Biological and Environmental Statistics*, 23, 509–528.

Zhang, L. C., Chambers, R. L. (2004), "Small Area Estimates for Cross-Classifications," *Journal of the Royal Statistical Society: Series B (Statistical Methodology)*, 66, 479–496.